Near-Room-Temperature Thermal Chemical Vapor Deposition of Poly(chloro-*p*-xylylene)/SiO_2 Nanocomposites

Jay J. Senkevich*,† and Seshu B. Desu

Department of Materials Science and Engineering, Virginia Tech, 213 Holden Hall, Blacksburg, Virginia 24061-0237

Received January 25, 1999. Revised Manuscript Received May 4, 1999

A great necessity exists to reduce power consumption, cross-talk, and RC delay in ultra-large-scale integration (ULSI) devices to further improve their performance by replacing SiO_2 with a low dielectric constant material. Recently, much work has been focused on chemical vapor deposition (CVD) polymer thin films; however, they often suffer from poor resistance to metal diffusion and undesirable dielectric anisotropy. To overcome these limitations, a thermal CVD nanocomposite consisting of poly(chloro-*p*-xylylene) (PPXC) and SiO_2 was developed utilizing a recently developed near-room-temperature thermal CVD method to deposit SiO_2. The composition of the nanocomposite thin films could be varied by increasing the vaporization temperature of the SiO_2 precursor, diacetoxy-di-*tert*-butoxysilane. Since the composition could be varied, both the index of refraction and the dielectric constant of the nanocomposites could potentially be varied, in situ, to deposit a graded film to eliminate the diffusion problem. The X-ray diffraction spectra show a reduction in the crystallinity of the nanocomposite with increasing weight fraction of SiO_2 compared to the PPXC homopolymer, thus reducing the dielectric anisotropy, resulting in a low in-plane capacitance desirable for ULSI devices. The thermal stability for the high polymer fraction (91%) nanocomposite was also better than that of the PPXC homopolymer at temperatures up to 415 °C after successive low-temperature postdeposition anneals in nitrogen. Microstructural analysis of a high weight fraction polymer nanocomposite, with transmission electron microscopy, revealed a continuous polymer phase with a largely interdispersed morphology on a ∼5−50-nm scale.

Introduction

A great interest exists to reduce power consumption, cross talk, and RC delay in ultra-large-scale integration (ULSI) devices by the introduction of a low dielectric constant interlayer dielectric. The prime candidate interlayer dielectrics to replace SiO_2 are polymeric materials, nanoporous silica, and amorphous carbon.[1−4] Nanoporous silica and amorphous carbon are developing rapidly. However, the development of polymeric materials are more advanced to include a viable thermal chemical vapor deposition (CVD) process where homopolymers, copolymers, and cross-linked copolymers with improved thermal and dielectric properties may be deposited.[1,5−7] Further, CVD is the most appropriate method to deposit interlayer dielectrics because of the film's high purity, conformality, reproducibility, and its potentially high manufacturing throughput. However, two concerns exist which need to be overcome to integrate polymeric materials. Metals such as copper can easily diffuse into polymers and therefore a barrier layer such as SiO_2 will be needed; and most CVD homopolymers exhibit a large dielectric anisotropy, resulting in a large in-plane capacitance negatively impacting the potential benefits for introducing polymeric materials.[8−10]

Thermal CVD nanocomposite thin film materials were developed to overcome these potential integration issues. The method used to the deposit the thermal CVD nanocomposites is a relatively simple one utilizing common well-characterized precursors for both the poly(chloro-*p*-xylylene) (PPXC) and SiO_2 constituents. The precursors are vaporized and chemically modified separately and only mixed before deposition. Since they are separate until just before deposition, the nanocomposite thin film's composition can be varied and thus its dielectric constant can be varied in situ. This reduces the number of separate processing steps of having to separately deposit the polymer and then the barrier layer. Further, the presence of SiO_2 disrupts the crystallinity of the polymer, reducing its anisotropy and

† Current address: ACT-Micro Devices, 7586 Old Peppers Ferry Loop, Radford, VA 24141.

(1) Lu, T.-M.; Moore, J. A. *MRS Bull.* **1997**, *22* (10), 28.
(2) Senkevich, J. J.; Desu, S. B. *Appl. Phys. Lett.* **1998**, *72* (2), 258.
(3) Jin, C.; Luttmer, J. D.; Smith, D. M.; Ramos, T. A. *MRS Bull.* **1997**, *22* (10), 39.
(4) Endo, K.; Tatsumi, T. *Appl. Phys. Lett.* **1996**, *68* (20), 2864.
(5) Gaynor, J. F.; Desu, S. B. *J. Mater. Res.* **1994**, *9* (12), 3125.
(6) Gaynor, J. F.; Senkevich, J. J.; Desu, S. B. *J. Mater. Res.* **1996**,*11* (7), 1842.
(7) Taylor, K. J.; Eissa, M.; Gaynor, J. F.; Jeng, S.-P.; Nguyen, H. *Mater. Res. Soc. Symp.* **1997**, *476*, 197.
(8) Senkevich, J. J.; Desu, S. B. *Semicond. Int.* **1998**, *21* (6), 151.
(9) Senkevich, J. J.; Simkovic, V.; Desu, S. B. *Mater. Res. Soc. Symp. Proc.* **1998**, *511*, 139.
(10) Ryan, E. T.; McKerrow, A. J.; Leu, J.; Ho, P. S. *MRS Bull.* **1997**, *22* (1), 49.

10.1021/cm990042q CCC: $18.00
Published on Web 06/19/1999

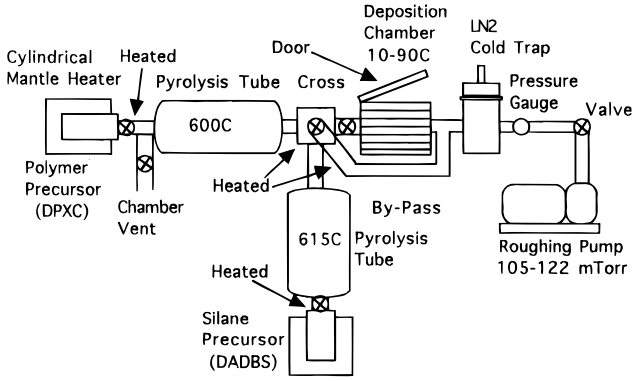

Figure 1. Custom-built CVD reactor with separate arms for SiO_2 and polymeric thin films.

hence the in-plane capacitance for the nanocomposite. In addition, the potential ability to control the dielectric constant and index of refraction in situ for the nanocomposites will enable the thermal CVD nanocomposites to be used as graded index films, low dielectric constant films, optical waveguides, scratch resistance films which may be applied to opthalmological lenses, and antireflection films.

Until recently, the deposition of a thermal CVD nanocomposite composed of a parylene polymer and SiO_2 was not possible since SiO_2 needed to be deposited below the threshold temperature of the polymer. The threshold temperature is the temperature above which the deposition rate of the polymer is approximately zero and is a function of the molecular weight and molecular structure of the polymer repeat unit. Poly(dichloro-*p*-xylylene) (PPXD) has a threshold temperature of 130 °C, poly(chloro-*p*-xylylene) (PPXC) 90 °C, and poly(*p*-xylylene) (PPXN) 30 °C.[11] Both the deposition of near-room-temperature thermal CVD of SiO_2 and multilayer thin film structures composed of PPXC and SiO_2 have been deposited successfully as reported previously.[12,13] However, until now no attempt has been made to deposit a thermal CVD nanocomposite composed of PPXC and SiO_2.

Experimental Section

Figure 1 shows a schematic of the custom-built CVD reactor with separate sublimation/vaporization chambers, pyrolysis tubes for the ceramic and polymeric constituents of the nanocomposite films, and a near-room-temperature deposition chamber. The alkoxysilane precursor diacetoxydi-*tert*-butoxysilane (DADBS) was placed in the vaporization chamber at 69−89 °C and the poly(chloro-*p*-xylylene) precursor DPXC (dichloro-*p*-xylylene or the cyclophane precursor) was placed in the sublimation chamber and heated to 116−119 °C. The DADBS and the DPXC pyrolysis chambers were heated to 615 and 600 °C to convert the precursors into their respective reactive intermediates. The SiO_2 thin film itself was pyrolyzed at 650 °C to test for impurity incorporation. The depositions typically lasted 20−70 min at a base pressure of 0.105−0.120 Torr at a deposition temperature of ~82 °C. The substrates used for depositing the films were (111) silicon, which were etched in a 0.05% HF solution for 5 min to etch the native oxide, rinsed with deionized water, blown dry with nitrogen, and placed in the deposition chamber. The parylene polymers are generally not sensitive to the surface condition of the substrate; however, this is not true with SiO_2. Thus, a minimum of etching the Si(111) substrate in HF prior to deposition is imperative.

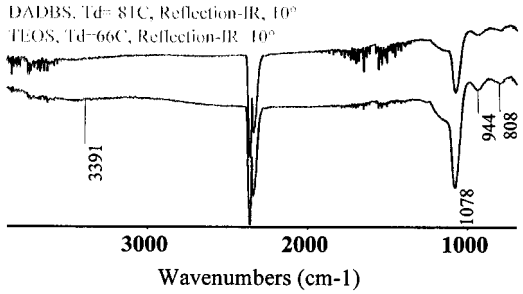

Figure 2. Reflection-FTIR spectrum of SiO_2 deposited from the silane alkoxy precursor DADBS at 81 °C and TEOS at 66 °C both taken 10° to the sample normal.

A Perkin-Elmer model 1600 FTIR was used for infrared spectroscopic measurements. A CaF_2 single-crystal substrate was used for the nanocomposite, SiO_2, and PPXC thin films. These films were analyzed from 4000 to 880 cm^{-1}. DADBS was analyzed from 4000 to 625 cm^{-1} after a neat cell consisting of NaCl single crystals was prepared. Quantitative analysis of the nanocomposite thin films was carried out by using wavelength dispersive X-ray analysis (WDXA). Duplicate samples using both Si(111) and titanium magnetron sputter coated Si(111) substrates were analyzed for quality assurance purposes. Thermal stability of PPXC and the 91 wt % PPXC nanocomposite thin films were analyzed by 1-h postdeposition anneals at successively higher temperatures in nitrogen. The change in thickness, indicative of weight loss, was measured by variable angle spectroscopic ellipsometry (VASE). X-ray diffraction data was obtained using a Scintag XDS-2000 X-ray diffractometer with Cu $K\alpha_1$ of 1.54059 Å. Scans were made from 10 to 26° 2θ at a scan rate of 2° 2θ/min for both PPXC and the nanocomposite films. Finally, transmission electron microscopy micrographs were obtained using a Phillips EM-620 TEM (transmission electron microscope). The filament current was 20 mA and the accelerating voltage 100 kV. PPXC and the nanocomposite were both grown directly on a copper TEM hexagonal grid, 600 mesh, hole diameter 14 μm. Both the polymer-rich nanocomposite and the homopolymer are able to grow transversely across the grid to form a thin film. However, the SiO_2-rich nanocomposite films are not able to do this; therefore, sample preparation would be more difficult.

Dielectric constant and loss were obtained by using a Solarton SI 1260 impedance analyzer. An alternating potential of 50 mV was applied to the sample. Both the top and bottom electrodes were physical-vapor-deposited (PVD) platinum and the top electrodes had a circular area of $3.42-3.53 \times 10^{-5}$ cm^2. A simple RC parallel circuit was used to calculate the capacitance and dielectric loss data at 10 kHz, 100 kHz, and 1 MHz. The thickness was measured by VASE and the electrode area by an optical microscope. In the case of the SiO_2 film, the thickness was 125 nm and the electrode area varied from 4.26 to 9.62×10^{-4} cm^2. Leakage current, electrical resistivity, and dielectric breakdown results were obtained using a Hewlett-Packard model 4140B pico amp/dc voltage source from 0 to 100 V.

SiO_2 and PPXC IR Characterization

IR spectroscopy qualitatively may be used to determine the chemical bonds present in a thin film material. Quantifying IR spectra is difficult since adsorption bands often show nonlinear behavior as a function of film thickness and some adsorption bands are much more intense than comparative bands in other materi-

(11) Beach, W. F.; Lee, C.; Bassett, D. R.; Austin, T. M.; Olson, R. A. In *Encyclopedia of Polymer Science & Technology*; Wiley: New York, 1989; Chapter 7, p 990.

(12) Senkevich, J. J.; Desu, S. B. *Adv. Mater.-CVD* **1998**, *10* (4), 92.

(13) Senkevich, J. J.; Desu, S. B. *Thin Solid Films* **1998**, *322* (1), 148.

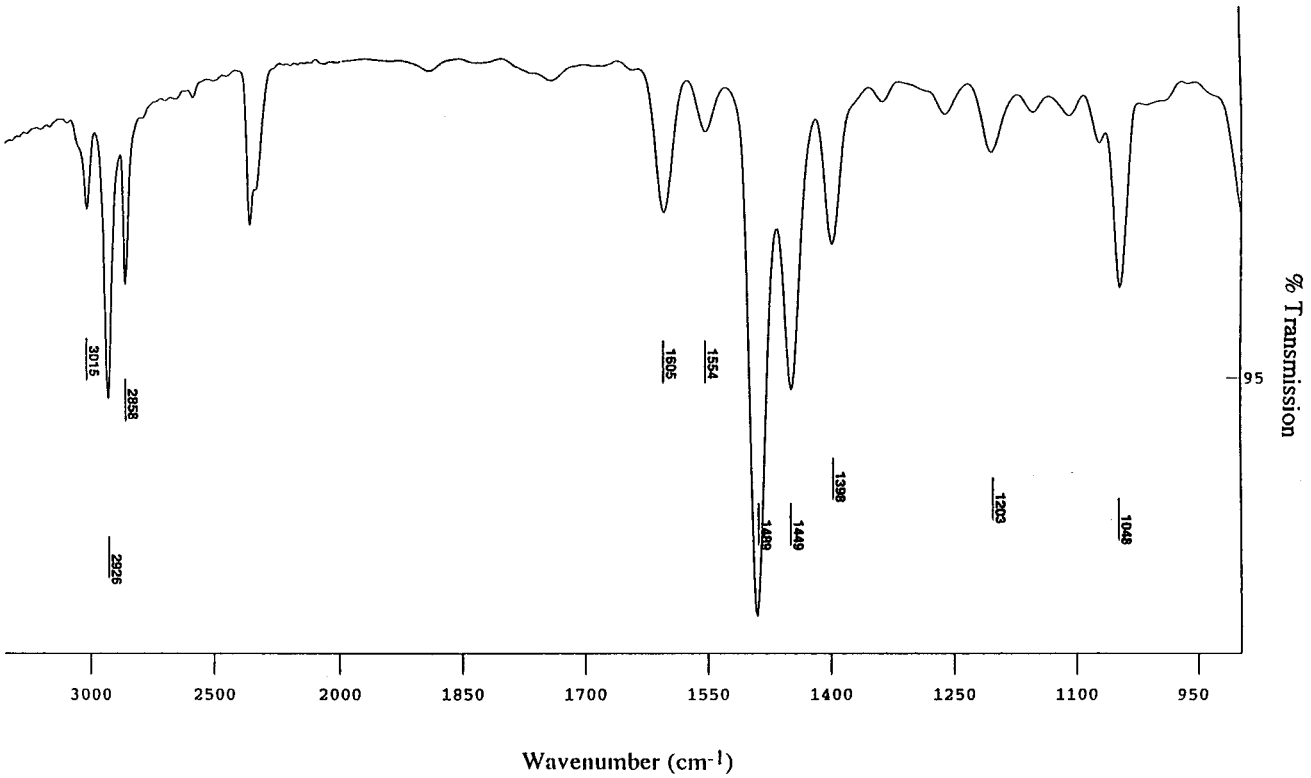

Figure 3. FTIR spectrum of poly(chloro-*p*-xylylene) (PPXC).

als. This section is included to enable later qualitative analysis of the thermal CVD nanocomposites to be more facile.

Only three peaks are present in Figure 3 for SiO_2 deposited from DADBS and tetraethoxysilane (TEOS) on Si(111) in reflection-IR mode 10° from the sample normal. The thermal CVD nanocomposite thin films developed here have utilized DADBS as a precursor because of its lower pyrolysis temperature; however, TEOS could also be used if so desired. The peak at 1078 cm^{-1} is due to the asymmetrical stretch of oxygen parallel to Si−O−Si, also called the transverse optical (TO) mode, whereas the much weaker peak at 808 cm^{-1} is due to the symmetrical stretch of oxygen parallel to Si−O−Si.[14] The peak at 1078 cm^{-1} may be deconvoluted into three separate peaks,[15] where the highest wavenumber broad peak which creates the characteristic asymmetrical hump results from either nonstoichiometry (SiO_x where $x < 2$) due to porosity or broken Si−O bonds to due to hydrolysis shifting the composite peak to lower wavenumbers.[15−17] The peak at 944 cm^{-1} is due to the Si−OH stretch and may also exist at 3200−3600 cm^{-1}; however, only a slight rise in the baseline exists there.

Figure 4 shows the transmission IR spectra of a 257-nm thin film of PPXC deposited on CaF_2 from 880 to 3200 cm^{-1}. Two sets of peaks are very characteristic of PPXC. The group 3015 cm^{-1} (aromatic), 2926 cm^{-1} (aliphatic), and 2858 cm^{-1} (aliphatic) are due to −CH stretching. The other set of distinguishing peaks for PPXC are at 1489, 1449, and 1398 cm^{-1} because of the C−H bending or deformation modes. The peaks at 1048 and 1605 cm^{-1} are characteristic of a 1,2,4-substituted phenyl group and aromatic C−C stretching, respectively. Finally, the peak at 2339 cm^{-1} is attributed to CO_2 and may be present at various intensities, depending on the extent of purging from the IR cell.

Deposition of the Thermal CVD Nanocomposite

The strongest evidence for the deposition of a nanocomposite material comes from transmission electron microscopy since PPXC and SiO_2 exhibit largely different electron-scattering powers, primarily because of their density differences, 1.289 g/cm^3 for semicrystalline PPXC and 2.2 g/cm^3 for SiO_2. Also, silicon and oxygen are larger atoms with larger electron-scattering cross sections as compared to carbon. Figure 4 shows an unstained bright-field TEM micrograph of PPXC shown at 432 800×. No distinguishing morphology is apparent, which is no surprise. However, the 57 wt % PPXC thermal CVD nanocomposite shown in Figure 5 at 229500× has strong morphological features. It shows a continuous polymer phase with interdispersed phases of PPXC (light areas) and SiO_2 (dark areas) from a ∼50-nm scale to below a ∼5-nm scale. It would be expected since SiO_2 is a network former, that it would be interdispersed into the polymeric domains as seen in Figure 5.

Other characteristic features of the thermal CVD nanocomposite as compared with PPXC and SiO_2 are shown in Table 1. The 91 wt % nanocomposite thin film exhibited a reduction in its birefringence, even with the slight reduction in crystallinity from 58% to 44% after a postdeposition anneal at 250 °C. The index of refrac-

(14) Lee, J. H.; Kim, D. S.; Lee, Y. H. *J. Electrochem. Soc.* **1996**, *143* (4), 1443.
(15) Goullet, A.; Charles, C.; Garcia, P.; Turban, G. *J. Appl. Phys.* **1993**, *74*, 6876.
(16) Pai, P. G.; Chao, S. S.; Takagi, Y.; Lucovsky, G. *J. Vac. Sci. Technol. A* **1986**, *4* (3), 689.
(17) Almeida, R. M.; Pantano, C. G. *J. Appl. Phys.* **1990**, *68*, 4225.

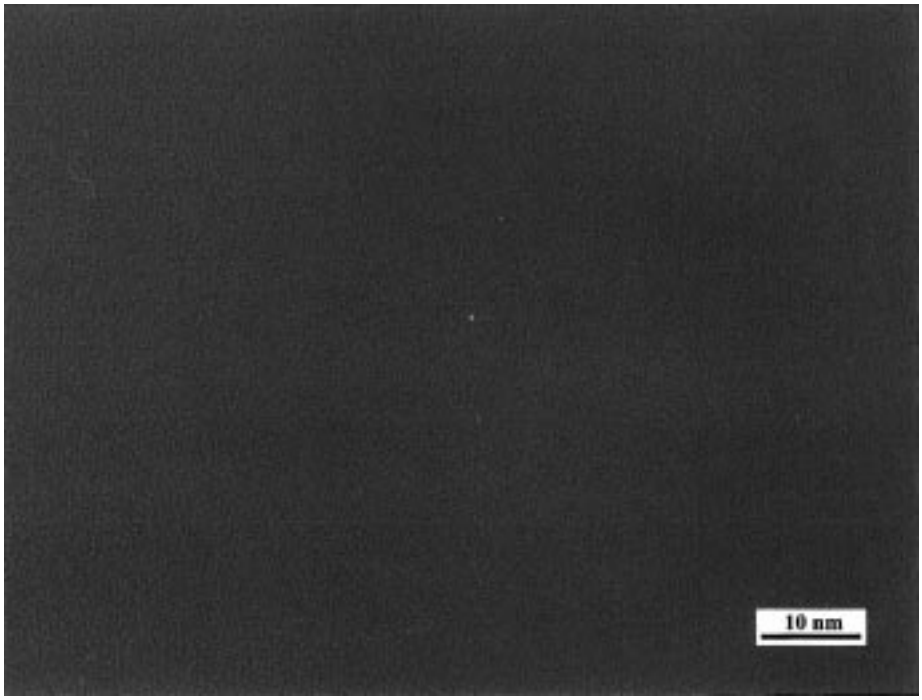

Figure 4. Transmission electron micrograph of poly(chloro-*p*-xylylene) at 432 800×.

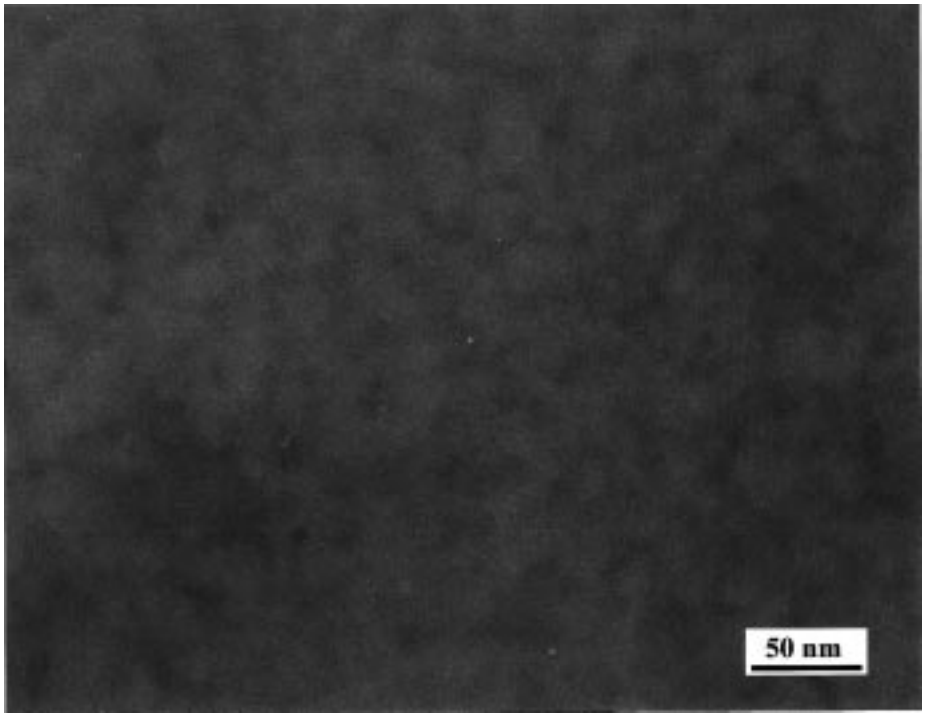

Figure 5. Transmission electron micrograph of the 57 wt % PPXC thermal CVD nanocomposite at 229 500×.

tion and the dielectric constant could also be varied, depending on the composition of the nanocomposite. The etch rate is an indirect indication of the morphology of the deposited thin film. The etch rate of the 91 wt % PPXC nanocomposite was 3.7 nm/min in a 1000:1 H_2O/HF solution. This was near the etch rate of PPXC, to be expected since the nanocomposite was mostly polymeric, but far away from the 19.1 nm/min etch rate of SiO_2. The deposition rate of the nanocomposite was 12.5 nm/min. The deposition rates of PPXC and SiO_2, at the same vaporization temperatures, were much lower, <1 and 2.5 nm/min. The deposition rate of the nanocomposite, however, is a function of the absolute and the ratio of vaporization temperatures of the precursors. The increase in the deposition rate of the thermal CVD nanocomposite as compared to that of the PPXC homopolymer or SiO_2 by themselves may indicate molecular interactions between the PPXC and SiO_2 reactive intermediates. However, this higher deposition rate could be simply a function of the increase pressure in the vicinity of the deposition chamber. The effect of deposition chamber pressure on the deposition rate of the nanocomposite and other films could not be easily studied since PPXC and SiO_2 can easily foul a nonheated capacitance manometer placed before the LN_2 cold trap. The nanoscale morphology seen in Figure 5

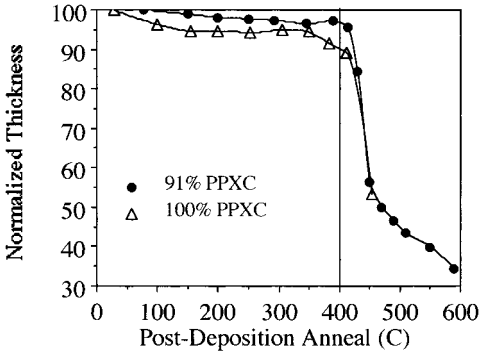

Figure 6. Thermal stability of the 91 wt % PPXC nanocomposite and PPXC homopolymer thin films as a function of successively higher post deposition anneals in nitrogen for 1 h each.

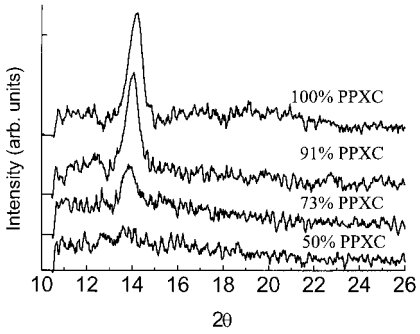

Figure 7. X-ray diffraction of thermal CVD nanocomposite composed of successively higher weight percentages of PPXC from bottom to top taken after at 250 °C anneal in nitrogen for 1 h.

Table 1. Nanocomposite versus PPXC and SiO_2 Characteristic Properties

	~91% PPXC nanocomposite	PPXC	SiO_2
n at 630 nm	1.624	1.639	1.432
Δ*n* at 630 nm (250 °C anneal)	0.0051	0.0216	isotropic
dielectric constant (1 MHz)	3.07	2.88	4.26
deposition rate	12.5 nm/min	<1 nm/min	2.5 nm/min
etch rate 1000:1 HF	3.7 nm/min	1.8 nm/min	19.1 nm/min
weight loss at 415 °C	4.4%	10.7%	<1%
crystallinity (250 °C anneal)	44%	58%	amorphous

is most likely due to the different mechanisms used to deposit the inorganic and organic components of the CVD nanocomposite. PPXC is deposited by a free-radical combination mechanism, whereas the deposition of SiO_2 via alkoxy silane precursors is debatable but may proceed by α-elimination, β-elimination, or a free-radical mechanism.[18,19]

The thermal stability of the 91 wt % nanocomposite was also improved over the PPXC homopolymer as measured at 415 °C in nitrogen and at every lower temperature as seen in Figure 6. The weight loss at 415 °C for the 91 wt % nanocomposite and PPXC homopolymer were 4.4% and 10.7%, nearly a 60% reduction. This reduction in weight loss may indicate that SiO_2 limits the diffusion of O_2 to the polymer chain, thus limiting

(18) Yasuda, Y. *Plasma Polymerization*; Academic Press: Orlando, FL, 1985; p 65.
(19) Desu, S. B. *J. Am. Ceram. Soc.* **1989**, *72*, 1615.

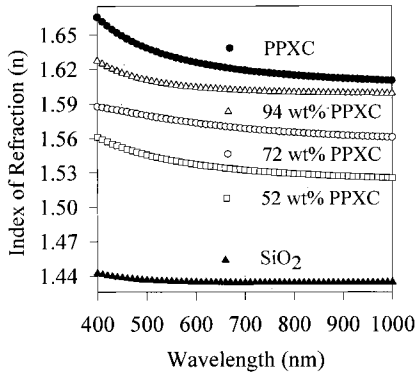

Figure 8. Control of the thermal CVD nanocomposite index of refraction as a function of its composition.

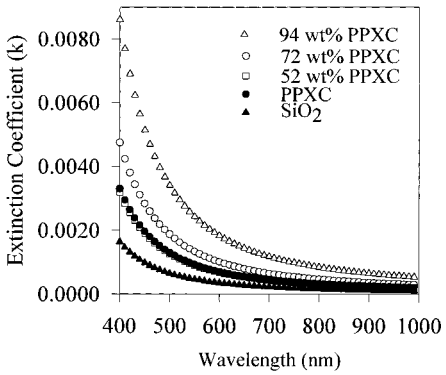

Figure 9. Change in the extinction coefficient as a function of the thermal CVD nanocomposite's composition.

Table 2. Electrical Properties of the CVD Nanocomposites

weight fraction PPXC	0.88	0.35	0.25
film thickness	257 nm	140 nm	162 nm
dielectric constant at 10 kHz	3.34	3.60	3.88
at 100 kHz	3.19	3.44	3.72
at 1 MHz	3.07	3.31	3.60
dielectric loss at 10 kHz	0.027	0.047	0.035
at 100 kHz	0.026	0.028	0.025
at 1 MHz	0.021	0.0267	0.0233
dielectric breakdown	>3.9 MV/cm	>7.1 MV/cm	>6.2 MV/cm
leakage current at 1 MV/cm	$<2.8 \times 10^{-11}$ A/cm^2	$<2.8 \times 10^{-11}$ A/cm^2	$<2.8 \times 10^{-11}$ A/cm^2
electrical resistivity at 1 MV/cm	$>3.5 \times 10^{16}$ Ω cm	$>3.5 \times 10^{16}$ Ω cm	$>3.5 \times 10^{16}$ Ω cm

the extent of degradation at temperatures >400 °C. However, both thin films exhibited rapid weight loss at ~450 °C because of the cleavage of the C−C aliphatic single bonds in the PPXC homopolymer. After the 490 °C nitrogen anneal for 1 h, no PPXC homopolymer film was left but the nanocomposite's weight loss leveled off because of the presence of the thermally stable SiO_2.

Compositional Control of the Thermal CVD Nanocomposites

The most important aspect in the development of the thermal CVD nanocomposite is the ability to control its composition in situ. For a polymeric material to be fully integrated into a typical IC, a diffusion barrier such as SiO_2 would have to be used because of the high diffusivity of metals, especially copper, into polymeric materials. This would add additional processing steps to the IC fabrication. On the other hand, the ability to

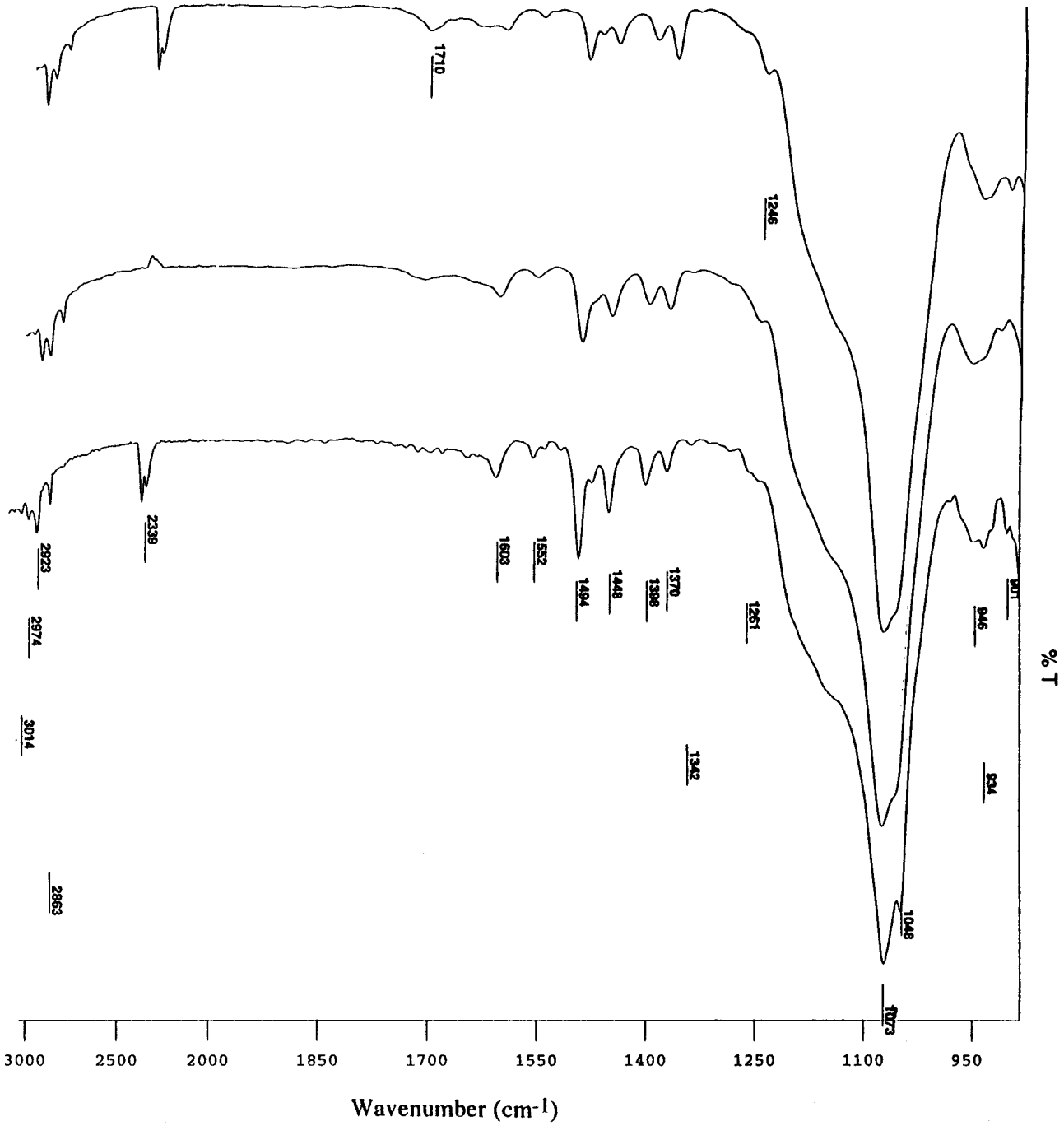

Figure 10. FTIR spectra of the thermal CVD nanocomposite thin films with increasing weight fraction of PPXC from top to bottom. Weight fraction PPXC: 0.24 (top), 0.57 (middle), and 0.84 (bottom).

deposit, in one step, a graded interlayer dielectric would require only one processing step.

The nanocomposite, with increasing weight percent SiO_2, exhibits a reduction in crystallinity as shown in Figure 7. A reduction in the degree of crystallinity is favorable since polymer crystallinity is the primary means by which the nanocomposite exhibits anisotropic dielectric properties.[8,9] PPXC exhibits positive birefringence which results in a low in-plane capacitance favorable for interlayer dielectrics to reduce parasitic capacitance.[20] However, most of the other parylene polymers are strongly negatively birefringent, poorly impacting their potential benefit for reducing cross talk, power consumption, and RC delay.

Increasing the fraction of SiO_2 in the nanocomposite increases PPXC's *d* spacing: 6.239, 6.295, and 6.367 Å for the 100%, 91%, and 73% PPXC thin films, respectively. The 50% PPXC nanocomposite has an even larger *d* spacing, but the peak is not well-defined and thus nearly amorphous. The larger *d* spacings mean that a less perfect crystal lattice unit cell is formed, which is reasonable if SiO_2 is present to disrupt polymer crystallization. The maximum obtainable percent crystallinity likewise decreases for the 100%, 91%, 73%, and 50% nanocomposites 58%, 44%, 14%, and ~0%, respectively. A more in-depth investigation into the structure of the

(20) Jeng, S.-P.; Havemann, R. H.; Chang, M.-C. *Mater. Res. Soc. Symp. Proc.* **1994**, *337* , 25.

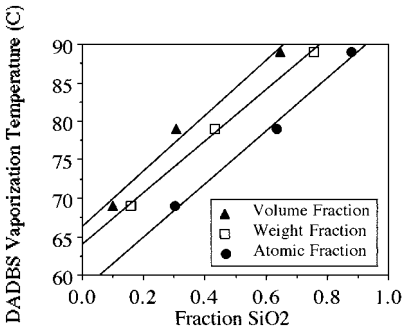

Figure 11. Wavelength dispersive X-ray analysis of the nanocomposite films at a deposition temperature of ~82 °C.

CVD nanocomposites will be published at a later date.

The most important property of the interlayer dielectric is its dielectric constant and associated electrical properties. Table 2 shows the electrical properties of three weight fractions of the thermal CVD nanocomposites. All three compositions exhibit a dispersion in their dielectric constants with increasing frequency. The high PPXC weight fraction nanocomposite exhibited a dielectric constant of 3.07 at 1 MHz and a loss of 0.021 which is nearly the same as PPXC (0.022). All three nanocomposites did not breakdown at 100 V and all three exhibited a leakage current below the detection limit of the pico amp meter at 1 MV/cm. All three CVD nanocomposites exhibited electrical properties much like PPXC in terms of their dielectric loss and leakage current.

In addition to being able to decrease the dielectric constant of the nanocomposite with increasing polymer content, the index of refraction increased with increasing polymer content as shown in Figure 8. The index of refraction could be varied from 1.436 at 630 nm for SiO_2 to 1.632 at 630 nm for PPXC. This could potentially lead to the development of optical waveguides, antireflection, and graded index thin films. Apparently, the dispersion in the index of refraction is reduced as the SiO_2 weight fraction is increased because of the lack of dispersion in SiO_2. The extinction coefficient versus wavelength is shown in Figure 9. As expected, the SiO_2 thin film exhibits the lowest extinction coefficient because of its intrinsic structure and its large band gap of 9 eV.[21] As seen with the dielectric loss data, the nanocomposites generally show a higher loss than either PPXC or SiO_2. This may be due to the small amount of byproducts present from the SiO_2 deposition or film roughness. After the 470 nm, 73 wt % nanocomposite thin film is annealed at 250 °C, the extinction coefficient dropped from 0.001 11 to 0.000 88 or 20% @630 nm. Higher postdeposition annealing and longer annealing times may liberate the pyrolysis byproducts, thus reducing the extinction coefficient. Further, the deposition of the CVD nanocomposites have not been fully optimized, and therefore lower values of extinction coefficient and dielectric loss should be expected.

Figure 10 shows three nanocomposite thin film spectra with an increasing weight fraction of PPXC from top to bottom (0.24, 0.56, and 0.84) by wavelength dispersive X-ray analysis (WDXA) as shown in Figure 11. The quality of the nanocomposite films chemically can be ascertained by IR spectroscopy. The nanocomposite IR spectra shows no evidence of the silane precursor DADBS. The major peak of DADBS according to Figure 12 is at 1747 cm^{-1}, which is absent in Figure 10. The two byproducts of DADBS are acetic acid and *tert*-butyl alcohol produced from the high-temperature pyrolysis reaction. The major adsorption peak of acetic acid is at 1710 cm^{-1} from the carbonyl group. Some acetic acid is

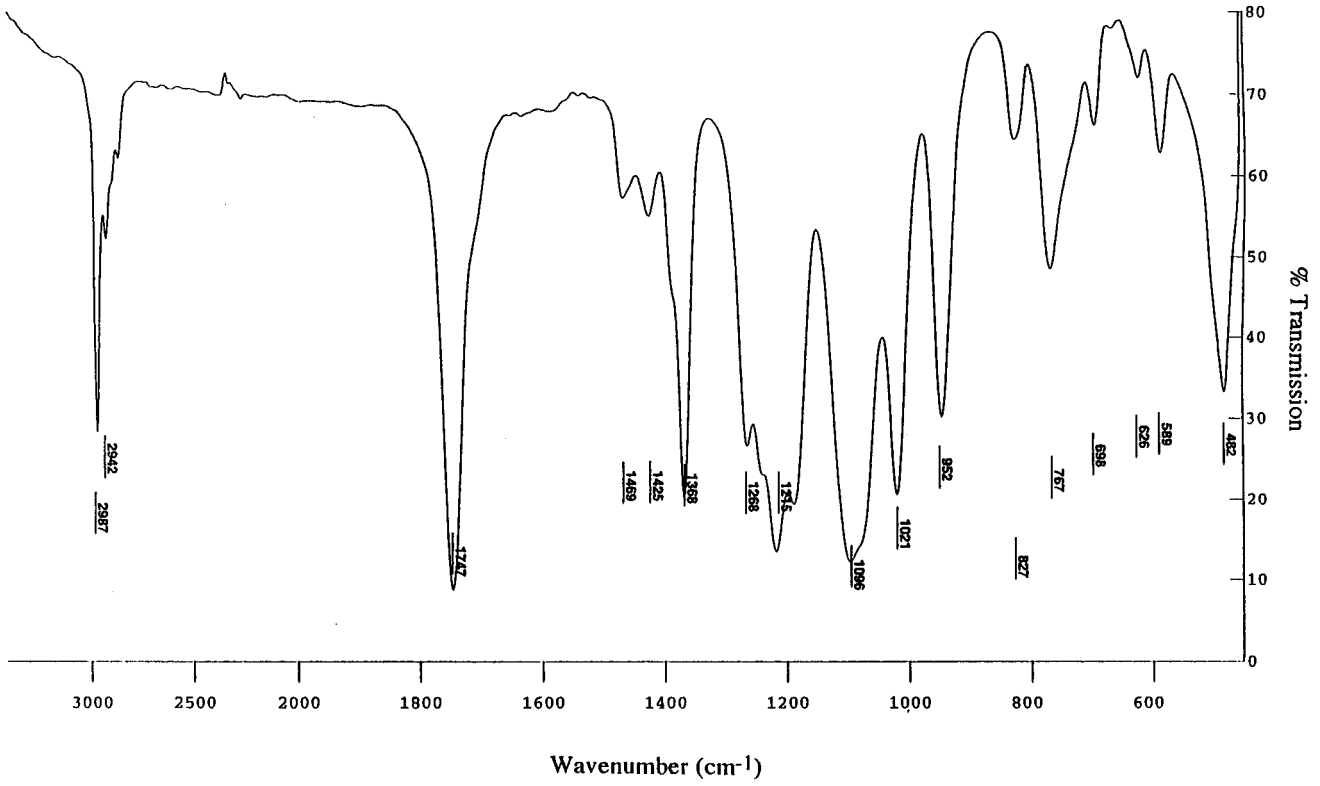

Figure 12. FTIR spectrum of diacetoxy-di-*tert*-butoxysilane (DADBS) prepared from a neat cell.

present in Figure 10 for the 24 wt % PPXC spectrum. However, the 54 and 84 wt % nanocomposite spectra lack acetic acid.

In contrast to acetic acid, *tert*-butyl alcohol is more abundant in the CVD nanocomposite IR spectra. Two *tert*-butyl alcohol peaks can be resolved and are distinguishable in Figure 10. The first is at 1370 cm^{-1}, because of the C−C stretch, and the second is at 2974 cm^{-1}, because of the C−H bending. As the weight percent of PPXC in the nanocomposite increases, these two peaks diminish in intensity. Since *tert*-butyl alcohol has a boiling point of 83 °C and acetic acid has one of 117−8 °C, it would be expected that acetic acid with its lower vapor pressure would be the dominant impurity. However, Hofman's proposed mechanism for the pyrolysis of DADBS liberates acid anhydride at $T > 200$ °C and 2-methylpropene at $T > 400$ °C, which become acetic acid and *tert*-butyl alcohol when exposed to water vapor postdeposition.[22,23] Therefore, to decrease the *tert*-butyl alcohol content in the film, an increase in the pyrolysis temperature is needed. This experiment was already undertaken with the SiO_2 thin film where the pyrolysis temperature for the FTIR spectrum in Figure 2 was 650 °C and shows neither acetic acid nor *tert*-butyl alcohol.

Conclusions

A nanocomposite composed of silicon dioxide and poly(chloro-*p*-xylylene) was deposited at ∼82 °C by a low-pressure thermal CVD method. The 91 wt % PPXC thermal CVD nanocomposite, as compared with the PPXC homopolymer and SiO_2, showed a much higher deposition rate at the same vaporization temperatures. The etch rate of the same composition in a 1000:1 H_2O/HF solution was reasonable at 3.7 nm/min as compared to a negligible etch rate of PPXC and the high etch rate of 19.1 nm/min for SiO_2. The 91 wt % PPXC nanocomposite exhibited a lower dielectric constant of 3.07 at 1 MHz and a higher index of refraction 1.624 at 630 nm as compared to SiO_2. Finally, the 91 wt % PPXC thermal CVD nanocomposite had a higher thermal stability than the PPXC homopolymer with a weight loss of 4.4% at 415 °C versus 10.7% after successive low-temperature postdeposition anneals. This result is encouraging for the future development of these thin film materials.

Equally important for the future development of these materials is the potential ability to control their composition in situ to fabricate graded films with a changing index of refraction or dielectric constant normal to the substrate. This, in combination with the nanocomposite's isotropic morphology compared with the currently available CVD homopolymers, may be valuable for future integration into ULSI devices. The drawbacks of using a polymer as an interlayer dielectric is mostly due to the high-diffusivity metals experience in polymers and the high in-plane capacitance most CVD homopolymers possess resulting from a large negative birefringence. The nanocomposites due to their in situ composition control can be deposited with a ∼100% SiO_2 layer at the metal interface, changing to a nearly 100% polymer in the center of the interlayer dielectric back to 100% SiO_2 at the other metal interface, thereby eliminating the diffusion problem and the need for a separately deposited barrier layer. This graded structure is easily obtainable with the use of mass flow controllers which may control the precursor feed rate.

CM990042Q

(21) Sze, S. M. *Physics of Semiconductor Devices*; John Wiley & Sons: New York, 1981.
(22) Hofman, R.; Westheim, J. G. F.; Haanappel, V. A. C.; Fransen, T.; Gellings, P. J. *Thermochim. Acta* **1993**, *215*, 329.
(23) Ashby, E. C.; Willard, G. F.; Goel, A. B. *J. Org. Chem.* **1979**, *44*, 1221.